SIAM J. NUMER. ANAL.
Vol. 44, No. 4, pp. 1466–1486

A PARALLEL METHOD FOR BACKWARD PARABOLIC PROBLEMS BASED ON THE LAPLACE TRANSFORMATION*

JINWOO LEE† AND DONGWOO SHEEN†

Abstract. A parallel method for time discretization of backward parabolic problems is proposed. The problem is reformulated to a set of Helmholtz-type problems with a parameter on a suitably chosen contour in the complex plane. After solving the resulting elliptic equations, which can be solved in parallel, we obtain a regularized solution with high frequency terms cut off by the inverse Laplace transforms without requiring the knowledge of the eigenfunctions of the differential operator. Since the regularized solution is obtained without artificial perturbation and high frequency components of the noise are suppressed, the quality of the solution is improved significantly compared to those obtained by other methods. Two different numerical inversions of Laplace transforms, with an arbitrary high order of accuracy and spectral accuracy, respectively, are used. Error estimates and numerical examples are presented.

Key words. numerical method, backward parabolic, ill-posed problem, Laplace transform, quadrature, parallel method

AMS subject classifications. 65N30, 35R25

DOI. 10.1137/050624649

1. Introduction.

We consider the following backward parabolic problem: given $u_0 \in L^2(\Omega)$, find $u = u(t) = u(\cdot, t) \in H_0^1(\Omega)$ such that

$$u_t + Au = 0 \quad \text{for } t \in (0, T], \quad \text{with } u(\cdot, 0) = u_0(\cdot) \text{ in } \Omega, \tag{1.1}$$

where $-A$ is a uniformly elliptic second-order partial differential operator on a domain Ω with a homogeneous Dirichlet boundary condition. Furthermore, we assume that A is a closed operator in the Hilbert space $L^2(\Omega)$ which generates an analytic semigroup $E(t) = e^{tA}$ and the spectrum $\sigma(-A)$ of $-A$ is contained in a sector $\{z \in \mathbb{C} : |\arg z| < \zeta\}$ for some $\zeta \in (0, \pi/2)$. We also assume that the resolvent $(zI + A)^{-1}$ of $-A$ satisfies

$$\|(zI + A)^{-1}\| \le \frac{C}{1 + |z|} \quad \text{for } z \in \Sigma_\zeta,$$

where the complementary sector Σ_ζ is given by

$$\Sigma_\zeta = \{z \in \mathbb{C} : \zeta < |\arg z| \le \pi\} \cup \{O\}.$$

Problem (1.1) is a well-known ill-posed problem in the sense that the solution does not depend continuously on the data u_0 [15, 19, 29]. However, it can be formulated as a well-posed problem, for instance, by imposing a prescribed bound on the solution at $t = T$ [19]. More precisely, given data $g \in L^2(\Omega)$ with noise, let $u^{(j)}$, $j = 1, 2$, be any two solutions of (1.1) satisfying

$$\|u^{(j)}(T)\| \le M \qquad \text{and} \qquad \|u_0^{(j)} - g\| \le \delta, \tag{1.2}$$

*Received by the editors February 17, 2005; accepted for publication (in revised form) February 16, 2006; published electronically July 31, 2006.
http://www.siam.org/journals/sinum/44-4/62464.html

†Department of Mathematics, Seoul National University, Seoul 151–747, Korea (jlee@nasc.snu.ac.kr, sheen@snu.ac.kr). The work of the second author was supported in part by Korea Research Foundation grant (KRF-2004-C00007).

where M and δ are given positive constants and $\|\cdot\|$ denotes the $L^2(\Omega)$-norm. Then it is known [29] that

$$\|u^{(1)}(t) - u^{(2)}(t)\| \le 2M^{t/T}\delta^{1-t/T} \quad \text{for } t \in (0, T], \tag{1.3}$$

which follows directly from the convexity of $F(t) = \log \|u^{(1)}(t) - u^{(2)}(t)\|^2$. We thus have continuous dependence on the data, and any numerical solution of the problem can be regarded as a kind of *regularized* solution depending on the two constraints M and δ in (1.2).

Stable numerical methods for backward parabolic problems can be applied to several practical areas such as image processing, mathematical finance, and physics. However, the ill-posedness nature of the problems requires certain types of regularization techniques. One approach to regularize the ill-posed problems is based on the use of eigenfunction expansion [17, 28, 23, 25, 30], where the eigenpairs of the corresponding elliptic operator are available. Another approach is to use the method of quasi reversibility [4, 7, 8, 12, 13, 14, 21, 27]. Other approaches include the least squares methods with Tikhonov-type regularization [2, 16, 18, 24, 26] and the use of heat kernel [9]. Buzbee and Carasso [4] introduced a method of transforming the problem (1.1) into a second-order in time problem. Later Carasso [5, 6] introduced the concept of a supplementary constraint such as that of slow evolution from the continuation boundary (SECB). The methods of quasi reversibility and Tikhonov regularization introduce artificial contamination, which is not from noises, to the numerical solutions. We thus expect to improve the solution quality if we can avoid any artificial perturbation and effectively suppress the influence of high frequency noises, which is the purpose of this paper. We also indicate that parallel algorithms have not yet been seriously addressed; however, see [24].

In this paper, we develop a parallel numerical method without any perturbation to obtain a regularized solution to problem (1.1). Instead of attacking problem (1.1) in the original space-time domain setting, we take the Laplace transform in time to have a set of complex-valued, Helmholtz-type problems with a parameter on a suitably chosen contour Γ in a control domain. After solving the resulting elliptic problems, the regularized time-domain solution with high frequency terms cut off can be recovered by applying the inverse Laplace transformation numerically. Two different choices of contour Γ will be described in detail in the next section. The first contour introduced in [32] requires no information on eigenpairs of the operator A, while the second one proposed in [22], which is more efficient, requires information on eigenvalues only. Since we obtain solutions without modifying the original problem and high frequency terms of noise are cut-off automatically, solution quality is improved significantly, especially as time goes on to the final time T (see the end of section 2.3).

The outline of the rest of the paper is as follows. In the next section, two numerical schemes are introduced based on the Laplace transformation of (1.1). In section 3, basic stability and error estimates are derived for these numerical schemes. Some numerical results are given in section 4.

2. The numerical schemes. Let us reformulate problem (1.1) by formally performing the Laplace transformation in time. Then

$$z\widehat{u} + A\widehat{u} = u_0 \text{ in } \Omega \quad \text{for } z \in \rho(-A) \tag{2.1}$$

with the homogeneous Dirichlet boundary condition on $\partial\Omega$, where $\rho(-A)$ is the resolvent set of $-A$. First, denote by $\{\phi_k\}_{k=1}^{\infty}$ and $\{\lambda_k\}_{k=1}^{\infty}$ the orthonormal eigenfunctions

of $-A$ and the corresponding eigenvalues which satisfy $0 < \operatorname{Re}\lambda_1 \le \operatorname{Re}\lambda_2 \le \cdots \to +\infty$. The solution $\widehat{u}(z)$ of (2.1) is then given in the following form:

$$\widehat{u}(z) = (zI + A)^{-1}u_0 = \sum_{k=1}^{\infty} \frac{1}{z-\lambda_k}(u_0, \phi_k)\phi_k, \tag{2.2}$$

since the solution of (1.1), if any, admits the representation

$$u(t) = \sum_{k=1}^{\infty} e^{\lambda_k t}(u_0, \phi_k)\phi_k. \tag{2.3}$$

In (2.3) we can observe that small errors on u_0 grow without bound, which is the source of ill-posedness. Among several regularization methods [17, 23] to avoid such an error growth, we shall employ a method of cutting off high frequency terms in the current paper.

From now on, denote by $\widehat{u}^{u_0}$ and $\widehat{u}^{g}$ the solutions to (2.1) with data u_0 and g, respectively. We begin by defining our regularization $u^{\Gamma,u_0}(t)$, using the Laplace inversion formula, by

$$u^{\Gamma,u_0}(t) = \frac{1}{2\pi \mathrm{i}} \int_{\Gamma} e^{zt}\widehat{u}^{u_0}(z)\, dz, \tag{2.4}$$

where, for some positive integer N,

$$\Gamma = \{z \in \mathbb{C} | \operatorname{Re}\lambda_N < \operatorname{Re} z < \operatorname{Re}\lambda_{N+1}\} \subset \rho(-A), \tag{2.5}$$

and the direction of Γ is taken such that $\operatorname{Im}(z)$ is increasing from $-\infty$ to $+\infty$. The contour Γ will be deformed subsequently for the sake of computational efficiency, and we will see that λ_i's need not be known explicitly for $\Gamma = \Gamma_1$ (see section 2.1 for the definition of Γ_1).

Notice that

$$\sum_{k=N+1}^{\infty} \frac{1}{z-\lambda_k}(u_0, \phi_k)\phi_k \text{ is analytic in the half plane left of the straight line contour } \Gamma,$$

which, incorporated into (2.2) and (2.4), implies that

$$\begin{aligned} u^{\Gamma,u_0}(t) &= \frac{1}{2\pi \mathrm{i}} \sum_{k=1}^{\infty} \int_{\Gamma} \frac{e^{zt}}{z-\lambda_k}(u_0, \phi_k)\phi_k\, dz \\ &= \frac{1}{2\pi \mathrm{i}} \sum_{k=1}^{N} \int_{\Gamma} \frac{e^{zt}}{z-\lambda_k}(u_0, \phi_k)\phi_k\, dz = \sum_{k=1}^{N} e^{\lambda_k t}(u_0, \phi_k)\phi_k, \end{aligned} \tag{2.6}$$

which is a spectral representation of $u^{\Gamma,u_0}(t)$ with high frequency terms cut off. The resulting $u^{\Gamma,g}(t)$ with a given data g satisfying (1.2) instead of u_0 fulfills the following stability condition:

$$\|u(t) - u^{\Gamma,g}(t)\| \le 2M^{t/T}\delta^{1-t/T} \quad \text{for } t \in (0, T] \tag{2.7}$$

if we choose N in (2.5) to be the largest integer such that

$$\operatorname{Re}\lambda_N \le \frac{1}{T}\log\frac{M}{\delta}$$

holds. See section 3 for more details.

2.1. The numerical procedure using a hyperbolic contour. We now deform the straight line contour Γ in (2.4) into the left-hand branch of a hyperbola, as in [32], with the asymptotes having slopes $\pm\kappa$, which crosses the real axis at $\gamma-\nu$, by setting

$$\Gamma_1 = \{z:\ z = z(\omega) = \sigma(\omega) + \mathrm{i}\kappa\omega,\ -\infty < \omega < \infty\} \subset \rho(-A), \qquad \sigma(\omega) = \gamma - \sqrt{\omega^2+\nu^2}, \tag{2.8}$$

for suitable parameters $\nu > 0$ (usually $\nu = 0.5$) and $\kappa > 0$, where γ will be chosen such that $\gamma - \nu = (1/T)\log(M/\delta)$, provided $\gamma-\nu$ does not coincide with any $\operatorname{Re}\lambda_i$. Then we have $\operatorname{Re}\lambda_N < \gamma-\nu < \operatorname{Re}\lambda_{N+1}$ for N used in Theorem 3.1. The parameters of Γ_1 are chosen such that the eigenvalues $\lambda_1,\dots,\lambda_N$ are to the left of the contour Γ_1, while the rest of eigenvalues are to the right of Γ_1. At the end of section 3.1 we will remark on the flexible choice of Γ_1. With the deformed contour Γ_1, the integral (2.4) can be written as

$$u^{\Gamma_1,u_0}(t) = \frac{1}{2\pi\mathrm{i}}\int_{-\infty}^{\infty} e^{z(\omega)t}\widehat{u}^{u_0}(z(\omega))z'(\omega)\,d\omega. \tag{2.9}$$

We notice that, as $\omega\to\pm\infty$, $e^{z(\omega)t}$ goes to zero rapidly, which accelerates convergence. Next, we transform the infinite interval $(-\infty,\infty)$ for ω in (2.9) into a finite one. For this, let $\psi:(-\infty,\infty)\to(-1,1)$ be defined by $\psi(\omega)=\tanh(\frac{\tau\omega}{2})$ as in [32]. In particular, by applying the change of variables $y=\psi(\omega)$ or, equivalently, $\omega = \psi^{-1}(y) = \frac{1}{\tau}\log\frac{1+y}{1-y}$ with the parameter $\tau>0$ to be determined later, the integral (2.9) can be transformed into one on $(-1,1)$ for y, where the trapezoidal rule can be applied to get

$$U^{\Gamma_1,u_0}_{L_1,\tau}(t) = \frac{1}{2\pi\mathrm{i}}\frac{1}{L_1}\sum_{j=-L_1+1}^{j=L_1-1} e^{z_jt}\widehat{u}^{u_0}(z_j)\frac{dz}{d\omega}(\omega_j)\frac{d\psi^{-1}}{dy}(y_j), \tag{2.10}$$

where

$$z_j = z(\omega_j),\quad \omega_j = \psi^{-1}(y_j) = \frac{1}{\tau}\log\frac{1+y_j}{1-y_j},\quad \text{and } y_j = \frac{j}{L_1},\ -L_1 < j < L_1. \tag{2.11}$$

The change of variables here spreads the equidistant points y_j's in $(-1,1)$ over $\mathbb{R}$ to ω_j's such that we have a finer grid near the origin where the integrand is relatively larger and a coarser grid where the integrand becomes relatively smaller. In [32], it is shown that this quadrature scheme has an arbitrary high order of accuracy for forward parabolic problems. In this paper we prove similarly that the same accuracy holds, although the properties of integrands are slightly different. The basic error estimate essentially shows that, for any positive integer r,

$$\|u^{\Gamma,u_0}(t) - U^{\Gamma_1,u_0}_{L_1,\tau}(t)\| \le \frac{C}{L_1^r}\left(\frac{\beta M}{\delta}\right)^{t/T}\|u_0\| \quad \text{for } t > r\tau, \tag{2.12}$$

where C depends on various parameters and $\beta>1$ is a constant.

2.2. The numerical procedure using a union of small circles. When the eigenvalues of the operator $-A$ are known, we can deform the contour in (2.4) into a union of disjoint small circles around the eigenvalues of $-A$ [22], which enables us

to reduce computational costs significantly when the number of dominant eigenvalues is relatively small. Set $d = \min_{1\le k\le N} \min_{l\neq k} |\lambda_k - \lambda_l|$ and assume that $d > 0$. For a sufficiently small $\varepsilon \in (0, d)$ (such that the circle $|z - \lambda_k| = \varepsilon$ contains no other eigenvalues than λ_k for all k), we define the second contour Γ_2 by

$$\Gamma_2 = \bigcup_{k=1}^{N} C_k \subset \rho(-A), \quad C_k = \{z : z = \lambda_k + \varepsilon e^{\mathrm{i}\theta}, 0 \le \theta \le 2\pi\}, \tag{2.13}$$

where N is again the largest integer such that $\operatorname{Re}\lambda_N \le (1/T)\log(M/\delta)$ holds. With this Γ_2, (2.4) can be written as

$$u^{\Gamma_2,u_0}(t) = \frac{1}{2\pi i}\sum_{k=1}^{N}\int_{C_k} e^{zt}\widehat{u}^{u_0}(z)\,dz. \tag{2.14}$$

After applying the change of variables $z = \lambda_k + \varepsilon e^{\mathrm{i}\theta}$ on each circle C_k and the trapezoidal rule, we have

$$U_{L_2}^{\Gamma_2,u_0}(t) = \frac{1}{2\pi}\sum_{k=1}^{N}\frac{2\pi}{L_2}\sum_{j=0}^{L_2-1} e^{z_{k,j}t}\widehat{u}^{u_0}(z_{k,j})\varepsilon e^{\mathrm{i}\theta_j}, \tag{2.15}$$

where $z_{k,j} = \lambda_k + \varepsilon e^{\mathrm{i}\theta_j}$ and $\theta_j = \frac{2\pi}{L_2}j$ for $0 \le j \le L_2 - 1$. The efficiency of this scheme originates in that the interval of the integral could be arbitrarily small by letting ε be small (it should not be too small because of the machine precision; see section 3.2). The error estimate of this scheme results in spectral accuracy of the form

$$\|U_{L_2}^{\Gamma_2,u_0}(t) - u^{\Gamma,u_0}(t)\| = C\left(\frac{\beta' M}{\delta}\right)^{t/T}\left(\varepsilon'^{L_2} + \frac{eps}{\varepsilon}\right)\|u_0\|, \tag{2.16}$$

where C is independent of ε and L_2, *eps* is the machine precision, and $\varepsilon' = \varepsilon/d$, for $\beta' = e^{\varepsilon T} > 1$. With a double precision calculation, *eps* can be as small as about 10^{-16}.

2.3. The fully discrete schemes. The fully discrete scheme is achieved by combining the time-discretization procedure, either (2.10) or (2.15), with the finite element method for spatial approximation procedure. For this, let $(V_h)_{h>0}$ denote a family of standard piecewise linear finite element subspaces of $H_0^1(\Omega)$. Let $a(\cdot,\cdot)$ be the natural sesquilinear form associated with A. Then the finite element approximation $\widehat{u}_h^{u_0}(z) \in V_h$ to the solution $\widehat{u}^{u_0}(z)$ of (2.1) satisfies

$$z(\widehat{u}_h^{u_0}(z), v) + a(\widehat{u}_h^{u_0}(z), v) = (u_0, v) \quad \forall v \in V_h, \forall z \in \rho(-A). \tag{2.17}$$

Thus the spatially discretized approximation U_h^{Γ,u_0} to u^{Γ,u_0} in (2.4) is given by

$$U_h^{\Gamma,u_0}(t) = \frac{1}{2\pi\mathrm{i}}\int_{\Gamma} e^{zt}\widehat{u}_h^{u_0}(z)\,dz. \tag{2.18}$$

By combining the time-discretization procedure, either (2.10) or (2.15), with the finite element method the fully discretized solution is given by either

$$U_{L_1,h,\tau}^{\Gamma_1,u_0}(t) = \frac{1}{2\pi\mathrm{i}}\frac{1}{L_1}\sum_{j=-L_1+1}^{j=L_1-1} e^{z_j t}\widehat{u}_h^{u_0}(z_j)\frac{dz}{d\omega}(\omega_j)\frac{d\psi^{-1}}{dy}(y_j) \tag{2.19}$$

or

$$U_{L_2,h}^{\Gamma_2,u_0}(t) = \frac{1}{L_2}\sum_{k=1}^{N}\sum_{j=0}^{L_2-1} e^{z_{k,j}t}\widehat{u}_h^{u_0}(z_{k,j})\varepsilon e^{\mathrm{i}\theta_j}, \tag{2.20}$$

respectively. If inexact data g is given, g will be used instead of u_0, which will be analyzed in section 3.

To conclude this section, let us indicate two special features of the proposed methods. First, the methods can be implemented in parallel in the main part, solving a set of elliptic equations (2.1), of the procedures without any essential data communication among processors since they are independent of each other. This idea goes back to [11, 10] for solving wave propagation problems in the space-frequency domain setting, and it was later applied to forward parabolic problems [31, 32] and to a forward integro-differential equation with positive memory [20]. Second, the methods proposed in the current paper do not introduce any perturbation from the original problem, unlike others [2, 4, 7, 8, 12, 13, 14, 16, 18, 24, 26, 30], and therefore the solution quality of our method is much better than that of others. The trick is in *formally* reformulating the problem into problems in the Laplace transformed setting as in (2.1). The reformulated equation (2.1) is well defined and well posed, although one cannot perform the Laplace transform of the solution (2.3) since it does not exist for any $z \in \mathbb{C}$. Thus we choose to start from this equation. When it is inverted by using the Laplace inversion formula (2.4), the contour Γ has to be selected, and it gives a natural way of controlling the frequency terms. Noticing that eigenvalues of $-A$ correspond to the poles of $\widehat{u}(z)$ (see (2.2)) we see that the poles to the left of Γ are taken and those to the right of Γ are discarded (see (2.6)). In this way the regularization is performed naturally without perturbing anything, and the high frequency components of noise whose eigenvalues are bigger than λ_N cause no influence on the numerical solutions. This feature improves the quality of the solutions remarkably, which will be illustrated in section 4.

3. Stability and error estimates. In this section we analyze the stability of and error estimates of the two numerical procedures introduced in the previous section. Before going into the details of both properties, we first state and prove an error estimate between the exact solution u of (1.1) with constraints (1.2) and the regularized solution $u^{\Gamma,g}$ in (2.4) with given data g satisfying (1.2).

THEOREM 3.1. *Let $g \in L^2(\Omega)$ be given. Suppose that u is an exact solution of* (1.1) *with constraints* (1.2). *If N in* (2.5) *is chosen to be the largest integer such that* $\operatorname{Re}\lambda_N \le (1/T)\log(M/\delta) < \operatorname{Re}\lambda_{N+1}$, *then the following error bound holds:*

$$\|u(t) - u^{\Gamma,g}(t)\| \le 2M^{t/T}\delta^{1-t/T} \text{ for } t \in (0,T]. \tag{3.1}$$

Proof. Let us consider the regularized solution with exact data u_0, say $u^{\Gamma,u_0}(t)$, and N be the largest integer such that $\operatorname{Re}\lambda_N \le (1/T)\log(M/\delta) \operatorname{Re}\lambda_{N+1}$. From (1.2) and (2.3), it follows that $\sum_{k=1}^{\infty} c_k^2 e^{2\operatorname{Re}\lambda_k T} \le M^2$ with $c_k = (u_0, \phi_k)$, and therefore

$$\begin{aligned}\|u(t) - u^{\Gamma,u_0}(t)\|^2 &= \sum_{k=N+1}^{\infty} c_k^2 e^{2\operatorname{Re}\lambda_k t} = \sum_{k=N+1}^{\infty} c_k^2 e^{2\operatorname{Re}\lambda_k t} e^{2\operatorname{Re}\lambda_k T} e^{-2\operatorname{Re}\lambda_k T}\\ &\le e^{2(t-T)\operatorname{Re}\lambda_{N+1}} \sum_{k=N+1}^{\infty} c_k^2 e^{2\operatorname{Re}\lambda_k T}\\ &\le (\delta/M)^{2(1-t/T)} M^2 = \delta^{2(1-t/T)} M^{2t/T}. \end{aligned} \tag{3.2}$$

Similarly, the difference between the two regularizations with initial data u_0 and g is estimated as follows: with $g_k = (g, \phi_k)$,

$$\|u^{\Gamma,u_0}(t) - u^{\Gamma,g}(t)\|^2 = \sum_{k=1}^{N}(c_k - g_k)^2 e^{2\,\mathrm{Re}\,\lambda_k t} \le e^{2\,\mathrm{Re}\,\lambda_N t}\sum_{k=1}^{N}(c_k - g_k)^2$$
$$\le (M/\delta)^{2t/T}\delta^2 = M^{2t/T}\delta^{2(1-t/T)} \tag{3.3}$$

since we have $\sum_{k=1}^{\infty}(c_k - g_k)^2 \le \delta^2$ by (1.2). The assertion is then obtained by the triangle inequality. ∎

3.1. Analysis of the numerical procedure using a hyperbolic contour. As we mentioned in section 2.1, we put $\gamma - \nu = (1/T)\log(M/\delta)$, provided it does not coincide with any λ_i. Let

$$\Sigma_{\zeta_1,\gamma-\nu} = \{z \in \mathbb{C} : \zeta_1 < |\arg(z - \gamma + \nu)| < \pi - \zeta_1\} \cup \mathcal{N}_{\gamma-\nu} \subset \rho(-A), \tag{3.4}$$

where $\mathcal{N}_{\gamma-\nu}$ is a neighborhood of $\gamma - \nu$ that does not contain any eigenvalue of $-A$, and $\zeta_1 \in (0, \pi/2)$ is chosen such that $\Gamma_1 \subset \Sigma_{\zeta_1,\gamma-\nu}$. By (2.2), we can find a constant $B_1 > 0$, independent of z, such that

$$\|(zI + A)^{-1}\| \le \frac{B_1}{1 + |z - \gamma + \nu|} \quad \text{for } z \in \Sigma_{\zeta_1,\gamma-\nu}. \tag{3.5}$$

We notice that $B_1 = O(\eta^{-1})$, where η is a distance between the two sets $\Sigma_{\zeta_1,\gamma-\nu}$ and $\sigma(-A)$, the spectrum of $-A$. From now on set $\beta = e^{\nu T}$. We then have the following stability estimate.

THEOREM 3.2. *Let $U_{L_1,\tau}^{\Gamma_1,g}$ be the approximation defined by* (2.10) *of the regularized solution $u^{\Gamma_1,g}$ given by* (2.9)*, with u_0 replaced by g. Then, for $t > \tau$,*

$$\|U_{L_1,\tau}^{\Gamma_1,g}\| \le C(\beta M/\delta)^{t/T}\|g\|,$$

where $C = \sqrt{2}(2 - \frac{1}{L_1})\sqrt{1+\kappa^2}B_1/(\tau\pi)$.

Proof. From (2.8), (2.10), and (2.11) it follows that

$$\|U_{L_1,\tau}^{\Gamma_1,g}(t)\| \le \frac{1}{2\pi}\frac{1}{L_1}\sum_{j=-L_1+1}^{L_1-1}|e^{z_j t}|\|\widehat{u}^g(z_j)\|\left|\frac{dz}{d\omega}(\omega_j)\frac{d\psi^{-1}}{dy}(y_j)\right|$$
$$\le \frac{\sqrt{1+\kappa^2}e^{\gamma t}}{\sqrt{2}\pi L_1}\sum_{j=-L_1+1}^{L_1-1}e^{-|\omega_j|t}\left|\frac{d\psi^{-1}}{dy}(y_j)\right|\|\widehat{u}^g(z_j)\|$$
$$\le \frac{\sqrt{1+\kappa^2}e^{\gamma t}}{\sqrt{2}\pi L_1}\sqrt{\sum_{j=-L_1+1}^{L_1-1}\left(e^{-|\omega_j|t}\frac{d\psi^{-1}}{dy}(y_j)\right)^2}\sqrt{\sum_{j=-L_1+1}^{L_1-1}\|\widehat{u}^g(z_j)\|^2} \tag{3.6}$$

since $\left|\frac{dz}{d\omega}(\omega_j)\right| \le \sqrt{2}$. Now, for $j \ge 0$,

$$e^{-|\omega_j|t}\frac{d\psi^{-1}}{dy}(y_j) = e^{-\frac{t}{\tau}\log\frac{1+y_j}{1-y_j}}\frac{2}{\tau}\frac{1}{1-y_j^2} = \frac{2}{\tau}\frac{(1-y_j)^{t/\tau-1}}{(1+y_j)^{t/\tau+1}} \le \frac{2}{\tau} \quad \text{if } t > \tau. \tag{3.7}$$

The same bound holds for $j < 0$. Since $\gamma = \log(M/\delta)/T + \nu$, we have

$$e^{\gamma t} = (\beta M/\delta)^{t/T}, \tag{3.8}$$

where we recall that $\beta = e^{\nu T}$. Next, by using (2.8) and (3.5), we have, for $z \in \Sigma_{\zeta_1,\gamma-\nu}$,

$$\begin{aligned}\|\widehat{u}^g(z(\omega))\| = \|(z(\omega)I + A)^{-1}g\| &\le \frac{B_1}{1+|z(\omega)-\gamma+\nu|}\|g\| \\ &\le \frac{B_1}{1+\kappa|\omega|}\|g\| \le B_1\|g\|, \end{aligned} \tag{3.9}$$

which, combined with (3.6), completes the proof. ∎

Our error analysis is based on an Euler–Maclaurin-type proposition [32].

PROPOSITION 3.3 (Sheen, Sloan, and Thomeé [32]). *Let $r \ge 1$ be given and assume that $v \in C^r(\mathbb{R}; L^2(\Omega))$ and*

$$\|v^{(j)}(\omega)\| = O(e^{-r\tau|\omega|}) \quad \text{for } j \le r \text{ as } |\omega| \to \infty.$$

Furthermore, if $\|v(\omega)\| = o(e^{-\tau|\omega|})$ for $r = 1$, then we have the error estimate

$$\|Q_{L_1,\tau}(v) - I(v)\| \le C_r \frac{1}{L_1^r}\left(1 + \frac{1}{\tau^r}\right)\int_{-\infty}^{\infty} e^{r\tau|\omega|}\sum_{j=0}^{r}\|v^{(j)}(\omega)\|\,d\omega,$$

where

$$I(v) := \int_{-\infty}^{\infty} v(\omega)\,d\omega \quad \text{and} \quad Q_{L_1,\tau}(v) := \frac{1}{L_1}\sum_{j=-L_1+1}^{L_1-1} v(\omega_j)\frac{d\psi^{-1}}{dy}(y_j). \tag{3.10}$$

The proof of Proposition 3.3 is given in [32].

Proposition 3.3 implies that the formula (3.10) is of an arbitrary high order of accuracy, provided $v(\omega)$ vanishes appropriately fast at infinity. Based on Proposition 3.3, we derive an error estimate between the regularized solution $u^{\Gamma_1,g}$ given in (2.4) and its time-discretized approximation $U^{\Gamma_1,g}_{L_1,\tau}(t)$ given in (2.10) using g instead of u_0.

LEMMA 3.4. *Let $u^{\Gamma_1,g}(t)$ and $U^{\Gamma_1,g}_{L_1,\tau}(t)$ be the regularized solution defined by* (2.4) *and its approximation defined by* (2.10)*, respectively, with initial data g instead of u_0 and r a positive integer. Then, for $t > r\tau$, we have*

$$\|u^{\Gamma_1,g}(t) - U^{\Gamma_1,g}_{L_1,\tau}(t)\| \le \frac{C_{r,t}}{L_1^r}\left(\frac{\beta M}{\delta}\right)^{t/T}\|g\|, \tag{3.11}$$

where $C_{r,t} = C_r\frac{(1+\kappa^2)^{r/2}}{k}(1+t^r)(1+\frac{1}{\tau^r})(1+\log_+\frac{\kappa}{t-r\tau})$ and $\log_+ x = \max(0,\log x)$.

Proof. Set $v(\omega,t) = \frac{1}{2\pi i}e^{z(\omega)t}\widehat{u}^g(z(\omega))z'(\omega)$. Then, from (2.9) and (2.10), with u_0 replaced by g, it follows that

$$u^{\Gamma_1,g}(t) - U^{\Gamma_1,g}_{L_1,\tau}(t) = I(v(\cdot,t)) - Q_{L_1,\tau}(v(\cdot,t)).$$

Our aim is to apply Proposition 3.3, and for this we need to bound the derivatives of the function $\widehat{u}^g(z)$ on Γ_1. Since $\frac{d^j}{dz^j}(zI+A)^{-1} = (-1)^j j!(zI+A)^{-j-1}$, (3.9) and an induction on j imply that

$$\left\|\frac{d^j}{dz^j}\widehat{u}^g(z)\right\| \le \frac{C_j}{1+\kappa|\omega|}\|g\| \quad \text{for } z \in \Gamma_1. \tag{3.12}$$

The Leibniz rule is then applied to obtain

$$\left\| \frac{\partial^j}{\partial \omega^j} v(t,\omega) \right\| \le C_r \left(1+t^r\right) \frac{(1+\kappa^2)^{r/2} e^{t\sigma(\omega)}}{1+\kappa|\omega|} \|g\| \quad \text{for } j \le r, \quad \omega \in \mathbb{R},$$

where $C_r > 0$ is a constant depending on $\|\frac{d^j}{d\omega^j}\sigma(\omega)\|_{L_\infty(\mathbb{R})}$ for $j \le r$. Since $\sigma(\omega) \approx -|\omega|$ for large $|\omega|$ the assumptions of Proposition 3.3 are thus satisfied if $t > r\tau$, and the proposition implies that

$$\|u^{\Gamma_1,g}(t) - U^{\Gamma_1,g}_{L_1,\tau}(t)\| \le C_r L_1^{-r} \left(1+\tau^{-r}\right)\left(1+t^r\right) e^{\gamma t} \int_{-\infty}^{\infty} \frac{(1+\kappa^2)^{r/2} e^{-|\omega|(t-r\tau)}}{1+\kappa|\omega|}\, d\omega\, \|g\|,$$

since we have $\sigma(\omega) \le \gamma - |\omega|$. To bound the integral that remains, notice that $\int_0^\infty e^{-\omega t}(1+\omega)^{-1}\, d\omega \le C(1+\log_+(1/t))$, which can be verified easily by arithmetic calculations. Then (3.8) is used to complete the proof of the lemma. ∎

Remark 3.5. The parameter r appears only in the theorem, not in the method. Its implication is that the larger the r, the faster the convergence. And the above estimate is valid at least for $t > \tau$. In the numerical examples in section 4, we choose $\tau = 1/2$.

Next we deal with the space-discretization error.

LEMMA 3.6. *Let $U^{\Gamma_1,g}_{L_1,\tau}(t)$ and $U^{\Gamma_1,g}_{L_1,h,\tau}(t)$ be defined as in* (2.10) *and* (2.19)*, respectively, using g instead of u_0. Then, for $t > \tau$, we have*

$$\|U^{\Gamma_1,g}_{L_1,\tau}(t) - U^{\Gamma_1,g}_{L_1,h,\tau}(t)\| \le Ch^2(\beta M/\delta)^{t/T}\|g\|, \tag{3.13}$$

where $C = C\sqrt{1+\kappa^2}\left(\frac{2L_1-1}{L_1\tau}\right)$.

Proof. Combining (2.10), (2.19), and (2.8) we have

$$\|U^{\Gamma_1,g}_{L_1,\tau}(t) - U^{\Gamma_1,g}_{L_1,h,\tau}(t)\| \le \frac{1}{2\pi}\frac{1}{L_1} \sum_{j=-L_1+1}^{L_1-1} |e^{z_j t}| \|\widehat{u}^g(z_j) - \widehat{u}^g_h(z_j)\| \left| \frac{dz}{d\omega}(\omega_j) \frac{d\psi^{-1}}{dy}(y_j) \right|$$

$$\le C\sqrt{1+\kappa^2}h^2\|g\| e^{\gamma t} \frac{1}{L_1} \sum_{j=-L_1+1}^{L_1-1} e^{-|\omega_j|t} \left| \frac{d\psi^{-1}}{dy}(y_j) \right| \tag{3.14}$$

since, for h small (see [33]),

$$\|\widehat{u}^g(z) - \widehat{u}^g_h(z)\| \le Ch^2\|g\| \qquad \text{for } z \in \Gamma_1.$$

Owing to (3.7),

$$\frac{1}{L_1} \sum_{j=-L_1+1}^{L_1-1} e^{-|\omega_j|t} \left| \frac{d\psi^{-1}}{dy}(y_j) \right| \le \frac{2}{\tau}\left(\frac{2L_1-1}{L_1}\right).$$

Then (3.8) is used to complete the proof. ∎

Finally, combining Theorem 3.1, Lemma 3.4, Lemma 3.6, and the triangle inequality, we obtain the main result of this subsection.

THEOREM 3.7. *Let $u(t)$ be an exact solution of* (1.1)*, $g \in L^2(\Omega)$ be given satisfying* (1.2)*, and $U^{\Gamma_1,g}_{L_1,h,\tau}(t)$ be our fully discretized approximation to $u(t)$ defined by* (2.19)*. Then we have, for any integer $r \ge 1$,*

$$\|u(t) - U^{\Gamma_1,g}_{L_1,h,\tau}(t)\| \le 2M^{t/T}\delta^{1-t/T}$$
$$+C\left(\frac{\beta M}{\delta}\right)^{t/T}\left(\frac{(1+\kappa^2)^{r/2}}{\kappa}\frac{1}{L_1^r} + \sqrt{1+\kappa^2}h^2\right)\|g\| \quad \textit{for} \quad r\tau < t < T.$$

Remark 3.8. The choice of contour Γ_1 is flexible by letting the parameter κ variable with the asymptotes having slopes ± 1 and the real axis cut at $\gamma - \nu$. Indeed, in (2.8), let $\kappa = \kappa(\omega)$ be chosen such that the contour Γ_1 can be nearly parallel to the imaginary axis until it meets the line $y = \pm \tan\zeta$ if the eigenvalue $\operatorname{Re}\lambda_{N-1}$ is close to $\operatorname{Re}\lambda_N$. Inside the sector Σ_ζ the contour can be deformed analytically to have asymptotes with slopes ± 1 in order to have fast convergence. Corresponding to the contour

$$\Gamma_1 = \{z : z = z(\omega) = \sigma(\omega) + \mathrm{i}\kappa(\omega)\omega, -\infty < \omega < \infty\} \subset \rho(-A),$$
$$\sigma(\omega) = \gamma - \sqrt{\omega^2 + \nu^2},$$

suitable modifications in the analysis can be carried out accordingly.

3.2. Analysis of the numerical procedure using a union of small circles. Let us turn to analyzing the case of the second numerical scheme under the assumption that the eigenvalues of $-A$ are known. We shall see that the quadrature scheme (2.15) with Γ_2 is of spectral accuracy. Since Γ_2 is a compact subset of $\rho(-A)$, we may assume that

$$\|(zI + A)^{-1}\| \le B_2 \quad \text{for } z \in \Gamma_2, \tag{3.15}$$

with B_2 independent of z. From (2.2) and (2.13) it follows that $B_2 = O(\varepsilon^{-1})$.

Set $\beta' = e^{\varepsilon T}$. We then have the following stability estimate.

THEOREM 3.9. *Let $U_{L_2}^{\Gamma_2,u_0}(t)$ be the approximation defined by* (2.15) *of the regularized solution* (2.14)*. Then we have*

$$\|U_{L_2}^{\Gamma_2,u_0}(t)\| \le CN(\beta' M/\delta)^{t/T}\|u_0\| \quad \textit{for } t > 0.$$

Proof. By using (2.2), (2.15), and (3.15), a direct estimation leads to

$$\left\|U_{L_2}^{\Gamma_2,u_0}(t)\right\| = \left\|\sum_{k=1}^{N}\frac{1}{L_2}\sum_{j=0}^{L_2-1} e^{z_{k,j}t}\widehat{u}(z_{k,j})\varepsilon e^{\mathrm{i}\theta_j}\right\|$$
$$\le B_2 N\varepsilon e^{(\lambda_N+\varepsilon)t}\|u_0\| \le CNe^{(\operatorname{Re}\lambda_N+\varepsilon)t}\|u_0\|,$$

owing to the fact $B_2 = O(\varepsilon^{-1})$. Finally, since $\operatorname{Re}\lambda_N \le \log(M/\delta)/T$, one has

$$e^{(\operatorname{Re}\lambda_N+\varepsilon)t} \le (\beta' M/\delta)^{t/T}, \tag{3.16}$$

which proves the theorem. ∎

Recalling that $d = \min_{1\le k\le N}\min_{l\ne k}|\lambda_k - \lambda_l|$ and $\varepsilon < d$ (see section 2.2), we have the following lemma.

LEMMA 3.10. *Let $u^{\Gamma_2,g}(t)$ and $U_{L_2}^{\Gamma_2,g}(t)$ be the regularized solution defined by* (2.14) *and its approximation defined by* (2.15)*, respectively, with g instead of u_0 and L_2 a positive integer. Then we have, for some $C > 0$ independent of ε and L_2,*

$$\|u^{\Gamma_2,g}(t) - U_{L_2}^{\Gamma_2,g}(t)\| \le CN\left(\frac{\beta' M}{\delta}\right)^{t/T}\left(\varepsilon'^{L_2} + \frac{eps}{\varepsilon}\right)\|g\| \quad \textit{for } t > 0, \tag{3.17}$$

where eps is the machine precision, and $\varepsilon' = \varepsilon/d$.

Proof. Let $F(z) = e^{zt}\widehat{u}^g(z)$. By (2.2), $F(z)$ has simple poles at $z = \lambda_k$ and thus has a Laurent series expansion of the form

$$F(z) = \sum_{m=-1}^{\infty} c_{k,m}(z-\lambda_k)^m \quad \text{for } |z-\lambda_k| < d, \tag{3.18}$$

where $c_{k,m} = \frac{1}{2\pi \mathrm{i}} \int_{C_k} \frac{F(z)}{(z-\lambda_k)^{m+1}}\, dz$. Due to Cauchy's residue theorem, we get

$$u^{\Gamma_2,g}(t) = \sum_{k=1}^{N} c_{k,-1}. \tag{3.19}$$

Plugging (3.18) into (2.15) with u_0 replaced by g and rearranging the summand, we have

$$\begin{aligned} U_{L_2}^{\Gamma_2,g}(t) &= \sum_{k=1}^{N} \frac{1}{L_2} \sum_{m=-1}^{\infty} c_{k,m}\varepsilon^{m+1} \left(\sum_{j=0}^{L_2-1} (e^{\mathrm{i}\theta_{m+1}})^j \right) \\ &= \sum_{k=1}^{N} \left(c_{k,-1} + c_{k,L_2-1}\varepsilon^{L_2} + c_{k,2L_2-1}\varepsilon^{2L_2} + \cdots \right). \end{aligned} \tag{3.20}$$

The last equality follows from the fact that if $m+1$ is a multiple of L_2, the sum with index j becomes L_2; otherwise, it is $\frac{1-(e^{\mathrm{i}\theta_{m+1}})^{L_2}}{1-e^{\mathrm{i}\theta_{m+1}}}$, which is 0. Under the assumption of no machine round-off error, one then has the following type of bound: $\|u^{\Gamma_2,g}(t) - U_{L_2}^{\Gamma_2,g}(t)\| \le CN\varepsilon^{L_2}$. However, the extra term eps/ε in (3.17) will be included due to the round-off errors which become significant if ε is too small. For the derivation of this and various examples which show the validity of this estimation, we refer the reader to [22].

Now we calculate $c_{k,m}$ explicitly to get the final error form. By inserting (2.2) into $c_{k,m}$, for $m \ge 0$, we get $c_{k,m} = (1/2\pi\mathrm{i}) \int_{C_k} G(z)/(z-\lambda_k)^{m+1} dz$, where $G(z) = \sum_{l\neq k} \frac{e^{zt}}{z-\lambda_l} g_l\phi_l$, and $g_l = (g, \phi_l)$. Notice that $G(z)$ is analytic inside C_k and recall the definition of d. Since $\beta' = e^{\varepsilon T} > 1$, we have, by Cauchy's integral theorem for derivatives, the Leibniz rule, and (3.16), that

$$\begin{aligned} \|c_{k,m}\| &= \frac{1}{m!}\|G^{(m)}(\lambda_k)\| = \left\| \sum_{r=0}^{m} \frac{1}{m!} \binom{m}{r} t^{m-r} e^{\lambda_k t} (-1)^r r! \sum_{l\neq k} \frac{g_l\phi_l}{(\lambda_k-\lambda_l)^{r+1}} \right\| \\ &\le t^m e^{\mathrm{Re}\,\lambda_N t} \left\| \sum_{r=0}^{m} \frac{t^{-r}}{(m-r)!} \sum_{l\neq k} \frac{g_l\phi_l}{|\lambda_k-\lambda_l|^{r+1}} \right\| \\ &\le t^m e^{\mathrm{Re}\,\lambda_N t} \frac{1}{d} \sum_{r=0}^{m} \frac{1}{(m-r)!} \left(\frac{1}{dt}\right)^r \|g\| \\ &= \frac{1}{d} e^{\mathrm{Re}\,\lambda_N t} \sum_{s=0}^{m} \frac{(dt)^s}{s!} \frac{1}{d^m} \|g\| \\ &\le \frac{1}{d^{m+1}} e^{dt} \left(\frac{\beta' M}{\delta}\right)^{t/T} \|g\| \quad \text{for } k \le N. \end{aligned} \tag{3.21}$$

The last estimate combined with (3.19) and (3.20) leads to

$$\begin{aligned}\|u^{\Gamma_2,g}(t) - U_{L_2}^{\Gamma_2,g}(t)\| &= \sum_{k=1}^{N}\sum_{m=1}^{\infty} \|c_{k,mL_2-1}\varepsilon^{mL_2}\| \\ &\le N\sum_{m=1}^{\infty}\left(\frac{\varepsilon}{d}\right)^{mL_2} e^{dt}\left(\frac{\beta' M}{\delta}\right)^{t/T}\|g\| \\ &= N\frac{(\varepsilon')^{L_2}}{1-(\varepsilon')^{L_2}} e^{dt}\left(\frac{\beta' M}{\delta}\right)^{t/T}\|g\| \\ &\le CN\left(\frac{\beta' M}{\delta}\right)^{t/T}\left(\varepsilon'^{L_2} + \frac{eps}{\varepsilon}\right)\|g\|,\end{aligned}$$

with $C = \frac{e^{dT}}{1-(\varepsilon')^{L_2}}$, where the machine precision truncation was considered in the last estimate. This completes the proof. ∎

Remark 3.11. Inequality (3.21) is the worst case estimate. Although there exist concrete examples that show that the above estimate is sharp, most experiments similar to the examples in section 4 exhibit that d acts as 1.

Remark 3.12. For a fixed L_2, we should have $(\frac{\varepsilon}{d})^{L_2} + \frac{eps}{\varepsilon} \ge 2(\frac{eps}{d})^{L_2/(L_2+1)}$ with equality holding for $\varepsilon = d^{L_2/(L_2+1)} eps^{1/(L_2+1)}$, which is an optimal choice of ε for a fixed L_2. With this ε the error bound tends to $C \cdot eps/d$ as L_2 tends to ∞.

Remark 3.13. In our case of computing $F(z)$ numerically, the smaller the ε one chooses, the more computational costs one needs in order to achieve a given tolerance. Thus Remark 3.12 says that any choice of ε and L_2 such that $(\varepsilon/d)^{L_2}$ is less than a given tolerance is economic, provided $\varepsilon > d^{L_2/(L_2+1)} eps^{1/(L_2+1)}$. In the examples in section 4 we regard d as 1.

Next we consider the space-discretization error.

LEMMA 3.14. *Using g instead of u_0, let $U_{L_2}^{\Gamma_2,g}(t)$ and $U_{L_2,h}^{\Gamma_2,g}(t)$ be as in* (2.15) *and* (2.20)*, respectively. Then we have*

$$|U_{L_2}^{\Gamma_2,g}(t) - U_{L_2,h}^{\Gamma_2,g}(t)\| \le CNh^2(\beta' M/\delta)^{t/T}\|g\| \quad for\ t > 0. \tag{3.22}$$

Proof. The lemma is a consequence of the estimate $\|\widehat{u}^g(z) - \widehat{u}_h^g(z)\| \le Ch^2\|g\|$ for $z \in \Gamma_2$ and Theorem 3.9 with u_0 replaced by g. ∎

We are, finally, in a position to state the main result of this subsection.

THEOREM 3.15. *Let $g \in L^2(\Omega)$ be given data satisfying* (1.2)*, $u(t)$ be an exact solution of* (1.1)*, and $U_{L_2,h}^{\Gamma_2,g}$ be the fully discretized approximation to $u(t)$ defined by* (2.20)*. Then we have*

$$\|u(t) - U_{L_2,h}^{\Gamma_2,g}(t)\| \le 2M^{t/T}\delta^{1-t/T} + CN\left(\frac{\beta' M}{\delta}\right)^{t/T}\left(\varepsilon'^{L_2} + \frac{eps}{\varepsilon} + h^2\right)\|g\|, \tag{3.23}$$

for $0 < t < T$, with $\varepsilon' = \varepsilon/d$.

Proof. The proof is just a combination of Theorem 3.1, Lemma 3.10, Lemma 3.14, and the triangle inequality. ∎

4. Numerical examples. Examples 1, 2, and 3 have been chosen to illustrate the convergence theory developed in section 3. The complicated solution profiles produced in Examples 4 and 5 demonstrate the high quality of the regularized numerical

solutions compared with that of other recently proposed numerical methods [2, 24]. Parallel performance is reported in Example 6.

In each example the initial data with noise are generated by adding a perturbation to the exact initial data. Let x_i, $1 \le i \le J$, be a uniform partition of Ω. For each i, let $rd(x_i)$ be a pseudorandom number selected from $(-1, 1)$. Then define $rd : \Omega \to [-1, 1]$ by linear interpolation of $rd(x_i)$ and set $per(x) := \delta \cdot rd(x)/|\Omega|^{d/2}$, where d and δ denote the dimension of Ω and amplitude, respectively.

Example 1. Let $\Omega = (0, \pi)$ and $T = 4$. Then consider the following backward parabolic problem:

$$u_t + u_{xx} = 0 \quad \text{in } \Omega \times (0, T), \tag{4.1a}$$

$$u = 0 \quad \text{on } \partial\Omega \times (0, T), \tag{4.1b}$$

$$u_0(x) = e^{-4} \sin x + e^{-16} \sin 2x \quad \text{for } x \in \Omega, \tag{4.1c}$$

with the exact solution $u(x, t) = e^{t-4} \sin x + e^{4(t-4)} \sin 2x$. Notice that the eigenpairs are $\phi_k = \sqrt{2/\pi} \sin kx$, and $\lambda_k = k^2, k = 1, 2, \ldots$. In this case we have $\|u(\cdot, T)\| = 1.89$. Set $M = 2$ and $\delta = 10^{-2}$ in (1.2). Then $\lambda_N \le (1/T) \log(M/\delta) = 1.32$, by which $\lambda_1 = 1$ is the largest eigenvalue bounded. Thus we have $N = 1$ in Theorem 3.1.

In implementation, (2.19) is applied with the contour Γ_1 given in (2.8) with the parameters chosen in the following fashion without requiring information on eigenpairs:

- we take $\nu = 0.5$ and $\tau = 0.5$;
- γ is chosen such that $\gamma - \nu = (1/T) \log(M/\delta) = 1.32$ at which the contour crosses the real axis; in this case, $\gamma = 1.82$.

In practice where the exact eigenvalues are not known, we recommend that γ is chosen such that $\gamma - \nu = (1/T) \log(M/\delta)$ if it does not coincide with any eigenvalue of $-A$. If $(1/T) \log(M/\delta)$ happens to be an eigenvalue of $-A$ (this occurs with probability 0), replace $(1/T) \log(M/\delta)$ with a slightly larger number so that it is not an eigenvalue and assign the resulting value as $\gamma - \nu$ to choose γ such that (3.4) is satisfied.

Now we would like to verify Theorem 3.1, or equivalently Theorem 3.7, provided the term $2M^{t/T}\delta^{1-t/T}$ is dominant. To use (2.19), $L_1 = 64$ and $h = \pi/600$ are chosen so that the term $2M^{t/T}\delta^{1-t/T}$ is dominant in (3.15).

TABLE 1

L^2 errors for Example 1: *actually computed L^2 errors and the predicted L^2 error bounds for $\delta = 10^{-2}$ and 10^{-4}.*

t	L^2 errors with $\delta = 10^{-2}$		L^2 errors with $\delta = 10^{-4}$	
	Computed	Predicted	Computed	Predicted
1	0.586E-02	0.752E-01	0.592E-04	0.238E-02
2	0.159E-01	0.283E+00	0.450E-03	0.283E-01
3	0.490E-01	0.106E+01	0.230E-01	0.336E+00
4	0.126E+01	0.400E+01	0.125E+01	4.000E+00

Table 1 shows the computational results for the L^2 errors and the error bounds, $2M^{t/T}\delta^{1-t/T}$, predicted by the Theorem 3.1. To illustrate the effects of different noise levels, we also showed errors with $\delta = 10^{-4}$, leaving the other parameters fixed except $\gamma = (1/T) \log(M/\delta) + \nu = 2.98$. Observe that the computational results in Table 1 are better than those predicted bounds by the theorem. However, it is well known [5, 17] that the estimate (3.1) is sharp, and one cannot improve this

without introducing a supplementary constraint such as that of slow evolution from the continuation boundary (SECB) [5, 6].

Example 2. In this example we report the L^2 error estimates for the first method (2.19) of time discretization to solve the same problem as in Example 1 with the data u_0 replaced by $u_0 = e^{-4}\sin x$ without adding noise. This enables the term $2M^{t/T}\delta^{1-t/T}$ in (3.15) to be neglected. In this case, $1/T\log(M/\delta)$ is infinity, which implies that the contour should contain all eigencomponents of the solution. The solution $u(x,t) = e^{t-4}\sin x$ contains 1 eigencomponent, and thus $\gamma - \nu$ should be greater than 1. Therefore we assigned $\gamma = 1.82, \nu = 0.5$, and $\tau = 0.5$ as in Example 1. Keeping the term $C(\beta M/\delta)^{t/T}/L_1^r$ to be dominant in (3.15) by choosing a sufficiently small $h(= \pi/5000)$, we vary L_1 to see the error behavior. Table 2 summarizes the L^2 errors. The values in the parentheses denote the error reduction ratios defined by $\log_2(e_{L_1/2}/e_{L_1})$, where e_{L_1} is the L^2 error with L_1 in (3.15). Notice that the rates of convergence, while erratic, are asymptotically as large as the order $t/\tau = 2t$ predicted by Theorem 3.7. That is, the error reduction ratios at time t become larger than $2t$ as L_1 is chosen sufficiently large.

TABLE 2
L^2 errors (and their reduction ratios) for Example 2.

$t\backslash L_1$	4	8	16	32
1.0	0.144E-02	0.645E-03(1.16)	0.305E-05(7.72)	0.419E-06(2.86)
2.0	0.120E-01	0.154E-02(2.97)	0.613E-05(7.97)	0.109E-07(9.13)
3.0	0.112E+00	0.196E-02(5.84)	0.192E-04(6.67)	0.455E-07(8.73)
4.0	0.842E+00	0.162E-01(5.70)	0.791E-04(7.68)	0.164E-06(8.91)

Example 3. Now we examine the second method (2.20) for the same problem as in Example 2. Thus parameters in (2.13) are chosen such that $N = 1$ and $\lambda_1 = 1$. Since the time-discretization errors for this method become small very rapidly, it is not easy to make the term $\varepsilon^{L_2} + eps/\varepsilon$ be dominant in (3.23). However, in [22] the theoretical and computational results have already been shown for this scheme without space variable to show the rate $\varepsilon^{L_2} + eps/\varepsilon$. In the current example, instead of varying ε and L_2, we thus fix $L_2 = 4$ and $\varepsilon = 10^{-2} > eps^{(1/L_2+1)} \approx 10^{-3}$ (see Remark 3.13) in (3.23) and vary h eight times smaller at each step which will reduce errors 1/64 times. This would verify that the space-discretization errors are dominant compared to their time-discretization counterparts.

TABLE 3
L^2 errors (and their reduction ratios) for Example 3.

$t\backslash h$	1/30	1/240	1/1920	1/15360
1.0	0.665E-04	0.976E-06(6.09)	0.154E-07(5.99)	0.510E-08(1.59)
2.0	0.330E-03	0.496E-05(6.05)	0.790E-07(5.97)	0.124E-07(2.67)
3.0	0.131E-02	0.200E-04(6.04)	0.328E-06(5.93)	0.202E-07(4.02)
4.0	0.471E-02	0.722E-04(6.03)	0.126E-05(5.84)	0.395E-07(5.00)

The numerical results in Table 3 provide confirmation of the behavior predicted by Theorem 3.15, where the predicted space-discretization error-reduction ratio is 6 since we choose h to be 1/8 times smaller at each step and the predicted time-discretization error $\varepsilon^{L_2} + eps/\varepsilon$ is about 10^{-8}. In the columns with $h = 1/240$ and $h = 1/1920$, the

apparent reduction ratios are more or less in agreement with the theory, while the ratios in the last column are less than 6 since the time-discretization errors, which are about 10^{-8}, are actively deteriorating the numerical solutions.

We now proceed to deal with two more complicated examples than the previous ones: the example employed in [24] which has severely oscillatory data and a similar example which appeared in [1, 2] with nonsmooth data. Consider the backward parabolic problem:

$$u_t + cu_{xx} = 0, \quad \Omega \times (0,T), \tag{4.2a}$$

$$u = 0, \quad \partial\Omega, \tag{4.2b}$$

with given noisy data $g \in L^2(\Omega)$. Let $\Omega = (0,l), l = 1$, or π. Here c is a positive constant that controls the diffusion speed. In this case, eigenvalues are $c(k\pi/l)^2, k = 1, 2, \ldots$. Thus when we apply Γ_2, in (2.13) $\lambda_k = c(k\pi/l)^2$, and N is chosen by the maximum integer k such that $c(k\pi/l)^2 \le (1/T)\log(M/\delta)$.

Example 4. Consider the problem (4.2) with $l = 1$, $T = 16$, $c = 1/87960$, and $u(x,T) = \sin(25\pi x^2)$. Since no analytic expression for u_0 is available, we solved a forward problem starting from $u(\cdot,T)$ using the method introduced in [32] to approximate u_0 as well as $u(\cdot,T/4), u(\cdot,T/2)$, $u(\cdot,3T/4), u(\cdot,7T/8)$, and $u(\cdot,15T/16)$, with errors less than 10^{-7}, which are served as reference solutions for (4.2).

The constant c is chosen so that the size of the oscillations in u_0 close to the right endpoint is less than 1 percent of that of $u(T)$ at the right endpoint. In [24], a similar data u_0 is used such that the size of oscillations in u_0 close to the right endpoint is less than 10 percent of their initial size. (Indeed, in [24] the constant $c = 1$ is used with very small time duration, with which the solutions agree with ours. Observe that any c and T in (4.2) give equivalent solutions if cT is constant.) Once u_0 is calculated, multiplicative noise is added (see Figure 1(c)) to make g such that $g = u_0(1 + per(x))$ with $\delta = 10^{-3}$, which should be stressed by comparing this with the choice $\delta = 10^{-6}$ in [24].

We have $\|u(\cdot,T)\| = M \approx 0.69$, and $(1/T)\log(M/\delta) \approx 0.41$. Thus when applying Γ_1, we choose $\nu = 0.5, \tau = 0.5$, and $\gamma = 0.91$. Also we used the discretization parameters $L_1 = 200$ and $h = 1/1000$. When we apply Γ_2, we choose $L_2 = 3, \varepsilon = eps^{1/(L_2+1)} \approx 10^{-4}$, and $h = 1/5000$. Figures 1(a) and 1(b) show the exact and the computed solutions at $t = T$ based on the contours Γ_1 and Γ_2, respectively.

Table 4 shows the predicted L^2 error bounds by Theorem 3.7 and the computed errors at various t values for the two contours Γ_1 and Γ_2. In order to compare with the method proposed in [24], computational results in [24] are also presented. The results from [24] are given in L^∞ errors, and thus we calculate L^∞ errors also in the parenthesis, although they are not much different since solutions are smooth.

We observe that the method [24] gives better results at $t = T/4$, but as we proceed to the final time our methods provide better solutions. Such an observation is expected for the following reasons. First, our methods recover information on eigenpairs without artificial contaminant since they do not perturb the original differential equation. Second, high frequency components of noise (larger than λ_N) do not affect our numerical solutions since they are automatically cut off in implementation.

We remark that the noise amplitude of our data g is 10^3 times as big as that in [24], and the loss of information on given data is worse than that of [24] by 10 times. With such a bad data our methods recover solutions relatively well.

We should also remark that the computed errors are much better than the predicted bounds given in Theorem 3.7. Even at $t = T$ when we lose continuous depen-

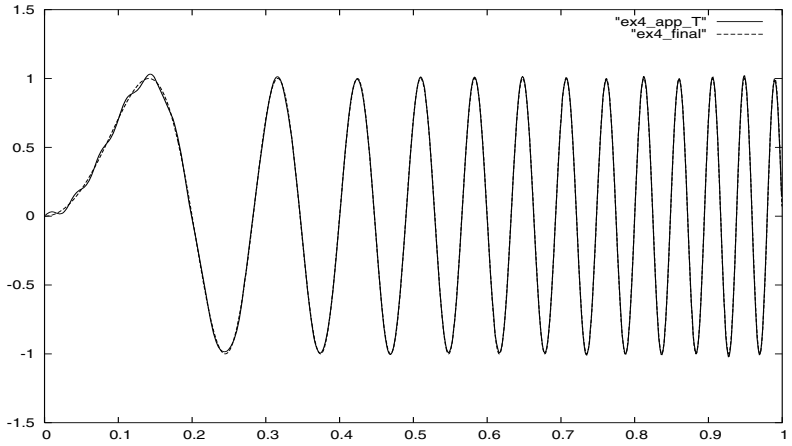

(a)

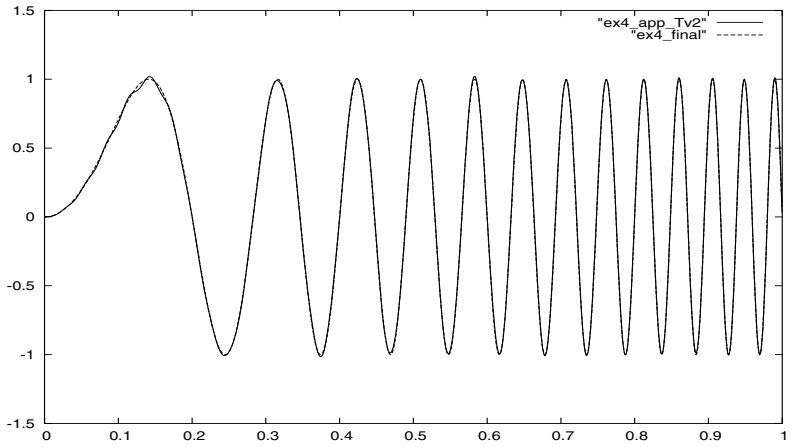

(b)

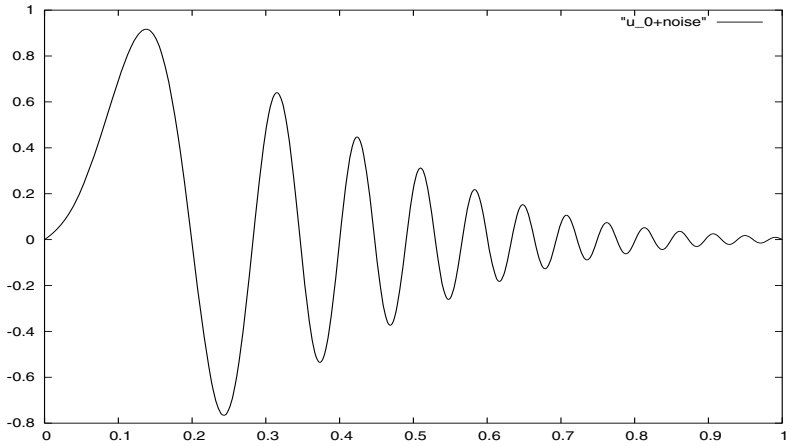

(c)

FIG. 1. (a) *Exact and computed solutions at* $t = T$ *using the contour* Γ_1, (b) *the contour* Γ_2, *and* (c) *the perturbed initial data profile with noise.*

TABLE 4
Comparison of errors for Example 4.

Time	Predicted errors	$L^2(L^\infty)$ errors using the contour Γ_1	$L^2(L^\infty)$ errors using the contour Γ_2	L^∞ errors from [24]
T/4	1.02E-02	1.56E-04 (6.83E-04)	1.46E-03 (2.42E-03)	6.25E-05
T/2	5.25E-02	5.88E-04 (2.16E-03)	1.57E-03 (3.64E-03)	1.09E-03
3T/4	2.69E-01	2.63E-03 (8.04E-03)	2.92E-03 (9.20E-03)	1.40E-02
7T/8	6.09E-01	5.71E-03 (1.62E-02)	5.65E-03 (1.69E-02)	4.44E-02
15T/16	9.16E-01	8.47E-03 (2.30E-02)	8.19E-03 (2.36E-02)	7.77E-02
T	1.38E+00	1.26E-02 (3.30E-02)	1.20E-02 (3.33E-02)	-

dence on the data theoretically, the computed L^∞ errors are of only 3.30 and 3.33 percent. This is typically the case when the diffusion coefficient is small, and the very high frequency components of the noise do not play a dominant role. This can be explained theoretically if we introduce further constraints, SECB [5, 6], which would be treated in a future work.

Finally, we would like to discuss our choice of $(c, T) = (1/87960, 16)$, which corresponds to $(c, T) = (1, 0.0001819)$. Although our T with $c = 1$ is bigger than that of [24], it is still small. While making "reasonable recovery," how large a T can one choose? It depends on the definition of "reasonable recovery" and which method one uses. Let us fix the L^2-norm of noises; say it is about 10^{-3}. We can say, for example, if the L^2 error of the recoverd image is less than 0.2, it is a "reasonable recovery." With our method, we can make $(c, T) = (1, 0.0002018)$. Recovered and the exact solutions are shown in Figure 2(a), where we observe highly tilted values as x approaches 1, which come from noises. Thus it is still challenging to make T as large as possible with such highly oscillating profiles.

Example 5. Now we consider (4.2) with $l = \pi$, $T = 4$, and $c = 1/32$, and the piecewise linear solution at $t = T$ given by

$$u(\cdot, T) = \begin{cases} 0, & 0 \le x \le \frac{\pi}{2}, \\ \frac{16}{\pi}x - 8, & \frac{\pi}{2} \le x \le \frac{3}{4}\pi, \\ 16 - \frac{16}{\pi}x, & \frac{3}{4}\pi \le x \le \pi. \end{cases} \tag{4.3}$$

As in Example 4, we integrate forward in time starting from $u(T)$ to generate u_0, $u(T/4)$, $u(T/2)$, and $u(3T/4)$, which are served as reference solutions for the problem. Additive noises are introduced by $g = u_0 + per$ with $\delta = 10^{-3}$. In this case $\|u(T)\| = M \approx 2.89$, and we choose $\gamma = (1/T)\log(M/\delta) + \nu \approx 2.49, L_1 = 100$, and $h = \pi/1000$ for Γ_1. For Γ_2 we take $L_2 = 4, \varepsilon = 10^{-2} > eps^{1/(L_2+1)} \approx 10^{-3}$, and $h = \pi/1000$. Table 5 shows L^2 errors, and Figure 2(b) presents the exact and the computed solution profiles at $t = T$ based on the contour Γ_1. Although the authors in [1, 2] stated a pessimistic opinion about approximating $u(T) \notin C^1$, our methods recover this profile in relatively good shape even with noisy data. The noise used for Example 5 is plotted in Figure 2(c).

Example 6. Finally, in order to observe the parallel performance of the proposed method, we solve a spatially three-dimensional (3D) problem version of (4.1)

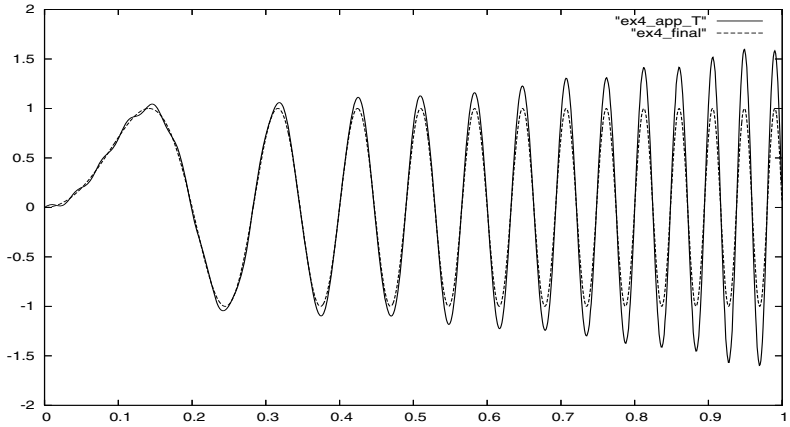

(a)

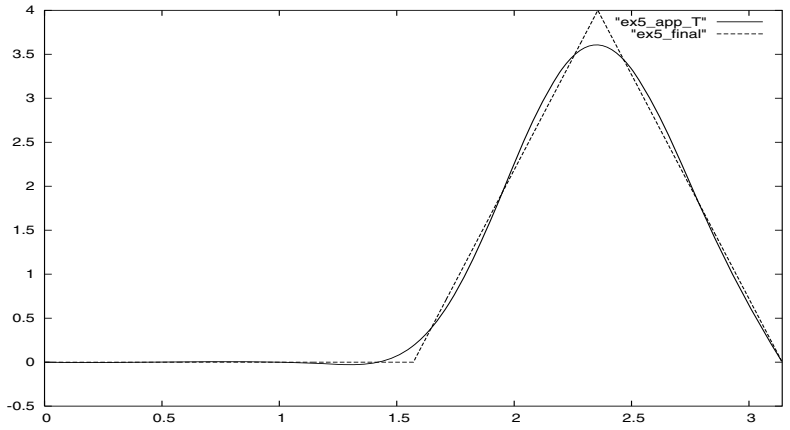

(b)

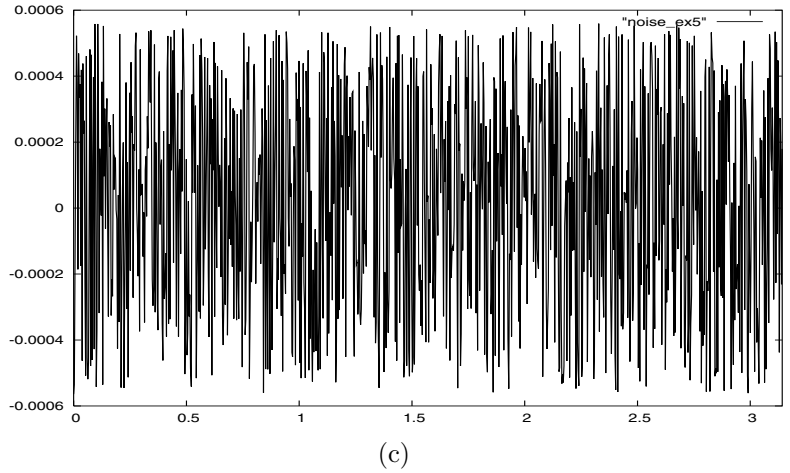

(c)

FIG. 2. (a) *Numerical and exact solutions with bigger* T *in Example* 4 *(*L^2 *error* $= 0.19$*),* (b) *profiles of computed and exact solutions of Example* 5 *using* Γ_1 *at* $t = T$*,* (c) *per*(x) *used for Example* 5.

TABLE 5
Predicted and computed errors for Example 5.

Time	Predicted errors	L^2 errors using the contour Γ_1	L^2 errors using the contour Γ_2
T/4	1.47E-02	7.05E-05	2.96E-04
T/2	1.08E-01	3.12E-04	8.51E-04
3T/4	7.89E-01	4.61E-03	7.13E-03
T	5.79E+00	1.48E-01	1.54E-01

TABLE 6
The computing time in seconds and speedup for Example 6. *The relative* $L^2(\Omega)$ *error of the approximation is* 5.99×10^{-3}.

# of processor(p)	1	2	4	8	16	32
Computing time	635.9	327.7	164.9	83.1	41.7	21.1
Speedup	1	1.9	3.9	7.7	15.2	30.1

$(\Omega = (0,1)^3$ and $T = 1)$ with $u_0(x) = \sin(\pi x)\sin(\pi y)\sin(\pi z)$. In this case, the exact solution is $u(x,t) = e^{3\pi^2 t}\sin(\pi x)\sin(\pi y)\sin(\pi z)$. For a fully discretized numerical solution, (2.19) is applied with $L_1 = 32$. $\gamma = 31.5$, and $\nu = \tau = 0.5$ are used for defining Γ_1 (see Example 2 for these selections). To obtain $\widehat{u}_h^{u_0}(z_j)$ $(j = 1, \ldots, L_1 - 1)$ in (2.19), we solved (2.1) using the Q_1-conforming (*e.g., trilinear*) finite element space V_h based on the $64 \times 64 \times 64$ uniform hexahedron triangulation of Ω (see, for instance, [3]). Then in order to calculate $U_{L_1,h,\tau}^{\Gamma_1,u_0}(1)$, p processors $(p = 1, 2, 4, 8, 16, 32)$ are employed to compute $L_1(=32)$ independent elliptic problems (2.1) for $z_j, j = 0, \ldots, L_1$, by evenly distributing them to p processors. For example if $p = 32$, each processor solves only one equation. The computing clock time in seconds from solving linear equations derived from (2.17) until obtaining $U_{L_1,h,\tau}^{\Gamma_1,u_0}(1)$ required with p processors are reported in Table 6. The speedup defined by (computing time for 1 processor)/(computing time for p processors) is also presented and a nearly perfect speedup is observed. The result is expected since the most time-consuming part in obtaining $\widehat{u}_h^{u_0}(z_j)$ for $j = 0, \ldots, L_1 - 1$ can be solved independently without data communication. Finally, we remark that obviously such a perfect speedup is expected when $p \leq L_1$. The computation of this example was carried out using a parallel machine whose nodes are based on the IBM PowerPC970 (2.2GHz) 2-way CPUs with 1 Giga Byte Myrinet network link.

5. Conclusion. In this paper, a parallel method has been proposed to solve backward parabolic problems. The algorithm is based on the Laplace transformation in time of the original time-dependent problems on a suitable contour in the complex plane. The time dependence of the resulting Laplace transformed problems is thus suppressed. After solving elliptic problems for each point on the complex contour, a numerical inversion of Laplace transformed solutions will recover the time-dependent solutions.

The proposed scheme to solve parabolic problems backwards in time does not introduce an artificial parameter in order to regularize the numerical solutions. Theories and numerical examples show the proposed method gives optimal stability without perturbing anything, resulting in improved quality of the regularized solutions.

Additionally our scheme is highly scalable for parallel implementaion in the realm of time discretization.

Acknowledgments. The authors wish to express thanks to the anonymous referees for their valuable suggestions to improve the original version. Thanks also go to Dr. Taeyoung Ha for providing a parallel 3D finite element code.

REFERENCES

[1] K. A. Ames, G. W. Clark, J. F. Epperson, and S. F. Oppenheimer, *A comparison of regularizations for an ill-posed problem*, Math. Comp., 67 (1998), pp. 1451–1471.

[2] K. A. Ames and J. F. Epperson, *A kernel-based method for the approximate solutions of backward parabolic problems*, SIAM J. Numer. Anal., 34 (1997), pp. 1357–1390.

[3] S. Brenner and R. Scott, *The Methematical Theory of Finite Element Methods*, Springer-Verlag, New York, 1994.

[4] B. L. Buzbee and A. Carasso, *On the numerical computation of parabolic problems for preceding times*, Math. Comp., 27 (1973), pp. 237–266.

[5] A. S. Carasso, *Overcoming Hölder continuity in ill-posed continuation problems*, SIAM J. Numer. Anal., 31 (1994), pp. 1535–1557.

[6] A. S. Carasso, *Logarithmic convexity and the "slow evolution" constraint in ill-posed initial value problems*, SIAM J. Math. Anal., 30 (1999), pp. 479–496.

[7] G. Clark and S. Oppenheimer, *Quasireversibility methods for nonwell-posed problems*, Electron. J. Differential Equations, 1994 (1994), pp. 1–9.

[8] D. Colton and J. Wimp, *The construction of solutions to the heat equation backward in time*, Math. Methods Appl. Sci., 1 (1979), pp. 32–39.

[9] J. Douglas, Jr., and J. R. Cannon, *The approximation of harmonic and parabolic functions on half-spaces from interior data*, in Numerical Analysis of Partial Differential Equations Symposium, Edizioni Cremonese, Rome, 1968, pp. 193–230.

[10] J. Douglas, Jr., J. E. Santos, and D. Sheen, *Approximation of scalar waves in the space–frequency domain*, Math. Models Methods Appl. Sci., 4 (1994), pp. 509–531.

[11] J. Douglas, Jr., J. E. Santos, D. Sheen, and Lynn S. Bennethum, *Frequency domain treatment of one–dimensional scalar waves*, Math. Models Methods Appl. Sci., 3 (1993), pp. 171–194.

[12] L. Elden, *Time discretization in the backward solution of parabolic equations.* I, Math. Comp., 39 (1982), pp. 53–68.

[13] L. Elden, *Time discretization in the backward solution of parabolic equations.* II, Math. Comp., 39 (1982), pp. 69–84.

[14] R. E. Ewing, *The approximation of certain parabolic equations backward in time by Sobolev equations*, SIAM J. Math. Anal., 6 (1975), pp. 283–294.

[15] J. Hadamard, *Lectures on the Cauchy Problems in Linear Partial Differential Equations*, Yale University Press, New Haven, CT, 1923.

[16] M. Hanke and P. C. Hansen, *Regularization methods for large-scale problems*, Survey Math. Indust., 3 (1993), pp. 253–315.

[17] W. Höhn, *Finite elements for parabolic equations backwards in time*, Numer. Math., 40 (1982), pp. 207–227.

[18] H. Houde and H. Gang, *Stabilized numerical approximations of the backward problem of a parabolic equation*, A Journal of Chinese Universities, 10 (2001), pp. 182–192.

[19] F. John, *Continuous dependence on data for solutions with a prescribed bound*, Comm. Pure Appl. Math., 13 (1960), pp. 551–585.

[20] K. Kwon and D. Sheen, *A parallel method for the numerical solution of integro-differential equation with positive memory*, Comput. Methods Appl. Mech. Engrg., 192 (2003), pp. 4641–4658.

[21] R. Lattes and J. L. Lions, *The Method of Quasi-Reversibility: Applications to Partial Differential Equations*, Elsevier, New York, 1969.

[22] J. Lee and D. Sheen, *An accurate numerical inversion of Laplace transforms based on the location of their poles*, Comput. Math. Appl., 48 (2004), pp. 1415–1423.

[23] P. Manselli and K. Miller, *Dimensionality reduction methods for efficient numerical solution, backward in time, of parabolic equations with variable coefficients*, SIAM J. Math. Anal., 11 (1980), pp. 147–159.

[24] J. M. Marbán and C. Palencia, *A new numerical method for backward parabolic problems in the maximum-norm setting*, SIAM J. Numer. Anal, 40 (2002), pp. 1405–1420.

[25] K. Miller, *Three circle theorems in partial differential equations and applications to improperly posed problems*, Arch. Rational Mech. Anal., 16 (1964), pp. 126–154.

[26] K. Miller, *Least squares methods for ill-posed problems with a prescribed bound*, SIAM J.

Math. Anal., 1 (1970), pp. 52–74.
[27] K. Miller, *Stabilized quasi-reversibility and other nearly-best-possible methods for nonwell-posed problems interior data*, in Proceedings of the Sympoisum on NonWell-Posed Problems and Logarithmic Convexity, Lecture Notes in Math. 316, Springer-Verlag, Berlin, 1973, pp. 161–176.
[28] K. Moszyński, *Approximation with frequency filter for backward parabolic equations*, Numer. Math., 88 (2001), pp. 159–183.
[29] L. E. Payne, *Improperly Posed Problems in Partial Differential Equations*, SIAM, Philadelphia, 1975.
[30] T. I. Seidman, *Optimal filtering for the backward heat equation*, SIAM J. Numer. Anal., 33 (1996), pp. 162–170.
[31] D. Sheen, I. H. Sloan, and V. Thomée, *A parallel method for time-discretization of parabolic problems based on contour integral representation and quadrature*, Math. Comp., 69 (2000), pp. 177–195.
[32] D. Sheen, I. H. Sloan, and V. Thomée, *A parallel method for time-discretization of parabolic equations based on Laplace transformation and quadrature*, IMA J. Numer. Anal., 23 (2003), pp. 269–299.
[33] V. Thomée, *Galerkin Finite Element Methods for Parabolic Problems*, Springer-Verlag, Berlin, 1997.